Dyes and Pigments 107 (2014) 9–14

Contents lists available at ScienceDirect

Dyes and Pigments

journal homepage: www.elsevier.com/locate/dyepig

Organic dyes containing 2-(1,1-dicyanomethylene)rhodanine as an efficient electron acceptor and anchoring unit for dye-sensitized solar cells

Carlos Alberto Echeverry [a], Alberto Insuasty [b], María Ángeles Herranz [b], Alejandro Ortíz [a], Robert Cotta [c], Vivek Dhas [c], Luis Echegoyen [c,*], Braulio Insuasty [a,**], Nazario Martín [b,d,***]

[a] Departamento de Química, Facultad de Ciencias Naturales y Exactas, Universidad del Valle, A.A. 25360 Cali, Colombia
[b] Departamento de Química Orgánica, Facultad de Química, Universidad Complutense, 28040 Madrid, Spain
[c] Department of Chemistry, University of Texas at El Paso, 79968-0519 El Paso, Texas, United States
[d] IMDEA-Nanoscience, Campus de Cantoblanco, Univerisdad Autónoma de Madrid, 28049 Madrid, Spain

ARTICLE INFO

Article history:
Received 24 January 2014
Received in revised form
4 March 2014
Accepted 8 March 2014
Available online 20 March 2014

Keywords:
Triphenylamine
Solar cells
Rhodanine
Anchoring unit
Electron acceptor
Dyes

ABSTRACT

Here we report the synthesis and characterization of five new organic dyes based on 2-(1,1-dicyanomethylene)rhodanine, which simultaneously serves as an efficient electron-acceptor moiety and anchoring unit to the TiO_2. Triphenylamine was used as the electron donor and a vinylthiophene unit was introduced to increase the pi-conjugation of the system and to widen the absorption region. The dye containing two 2-(1,1-dicyanomethylene)rhodanine units and no thiophene units showed the best photovoltaic performance with a short-circuit photocurrent density of 7.76 mA/cm^2, an open circuit photovoltage of 0.62 V, and a fill factor of 0.68, corresponding to an overall conversion efficiency of 3.78% under AM 1.5 irradiation (100 mW/cm^2).

1. Introduction

During the last few decades, finding new energy alternatives to fossil fuels has become a major challenge for the scientific community, and solar energy represents a highly promising renewable source [1]. Among the different types of solar cells, dye-sensitized solar cells (DSSCs) are moving to the forefront of the field, not only because of their relatively good efficiencies but also because they are cheaper than those based on silicon [2]. In a typical DSSC device, light is absorbed by the dye molecules which are anchored to the TiO_2 surface through carboxylic acid groups. Electrons from the excited state of the dye are then injected into the conduction band of the TiO_2, thus generating electric current [3]. So far, DSSCs show conversion efficiencies of light to electric power of up to 12.3% and have been obtained with polypyridyl ruthenium complexes and zinc porphyrin dyes [4]. Interest in metal-free organic sensitizers has grown in recent years because they offer some advantages over other sensitizers, these include higher molar absorption coefficients due to intramolecular $\pi-\pi^*$ transitions and easy modification due to relatively short synthetic routes, when compared with the conventional ruthenium based chromophores [5].

Sensitizers normally used in DSSCs feature donor–π bridge–acceptor (D–π–A) molecules. Several electron donor units such as porphyrins [6], *ex*TTFs [7] and triphenylamines [8], have been extensively investigated. An important observation is that the use of non-planar or bulky groups is critical in order to prevent dye aggregation, which favors the recombination of free charges, hence, a decrease in the device's efficiency. Triphenylamine (TPA) is a good candidate for this purpose [9,10]. On the other hand, different electron acceptors normally use a carboxylic acid (COOH) anchoring group for binding to the TiO_2. Nevertheless, it is worth mentioning that the COOH dissociates on the TiO_2 surface after long irradiation times, increasing the lability of these molecules [11]. Because of this, it is important to look for other kind of linkages that are able to bind strongly to the TiO_2. It has recently been reported

* Corresponding author. Tel.: +1 9157477573.
** Corresponding author. Fax: +57 2 3393248.
*** Corresponding author. IMDEA-Nanoscience, Campus de Cantoblanco, Univerisdad Autónoma de Madrid, 28049 Madrid, Spain. Fax: +57 2 3393248.
E-mail addresses: Echegoyen@utep.edu (L. Echegoyen), Braulio.insuasty@correounivalle.edu.co (B. Insuasty), Nazmar@quim.ucm.es (N. Martín).

http://dx.doi.org/10.1016/j.dyepig.2014.03.010
0143-7208/

that the synthesis of *push–pull* systems covalently attached to 2-(1,1-dicyanomethylene)rhodanine (DCRD) [12] allows efficient anchoring to the TiO_2 without the presence of the COOH group [13].

In this article, we report the synthesis and characterization of five new DCRD-based organic dyes (Scheme 1) and their further application as sensitizers in DSSCs. In our design, TPA aldehydes (**2**–**4**) were covalently linked to the DCRD by a Knoevenagel reaction. A vinylthiophene unit was introduced to bridge the donor and acceptor in order to increase the π-conjugation of the system. The combination of experimental results and density functional theory (DFT) calculations shows that the introduction of the π-bridge has a strong influence on the properties of the dyes.

2. Results and discussion

2.1. Synthesis of 2-(1,1-dicyanomethylene)rhodanine-based dyes

The preparation of the new *push–pull* chromophores was carried out using simple and straightforward synthetic routes. The rhodanine acceptor, (**5**), was prepared by a Knoevenagel condensation of rhodanine with malononitrile under basic conditions. The donor systems (**2**–**4**) were obtained in high yield from commercially available triphenylamine (**1**), using the Vilsmeier–Haack reaction [14]. The target molecules **DCR-(1–5)** were prepared in moderate to good yields (52–80%) by a Knoevenagel condensation of the active methylene compound **5** and the respective TPA aldehydes under microwave conditions (100 W, 60 °C and 30 PSI). The microwave radiation was used not only because it significantly reduces the reaction time from hours (12 h to prepare the **DCR-(1–5)**, approximately) to minutes, but it also increases the yields and improves reproducibility, compared to conventional refluxing. The synthetic procedures followed for the preparation of the **DCR** dyes are shown in Scheme 1. Aldehydes **7** and **8** were prepared by a Horner–Wadsworth–Emmons reaction of compounds **2** and **3** with diethyl 5-(1,3-dioxan-2-yl)-2-thienylmethylphosphonate (**6**) followed by the deprotection of each aldehyde group, which gave rise to the desired products in good yields (80–85%) [15]. The structures of the new compounds were supported by their analytical and

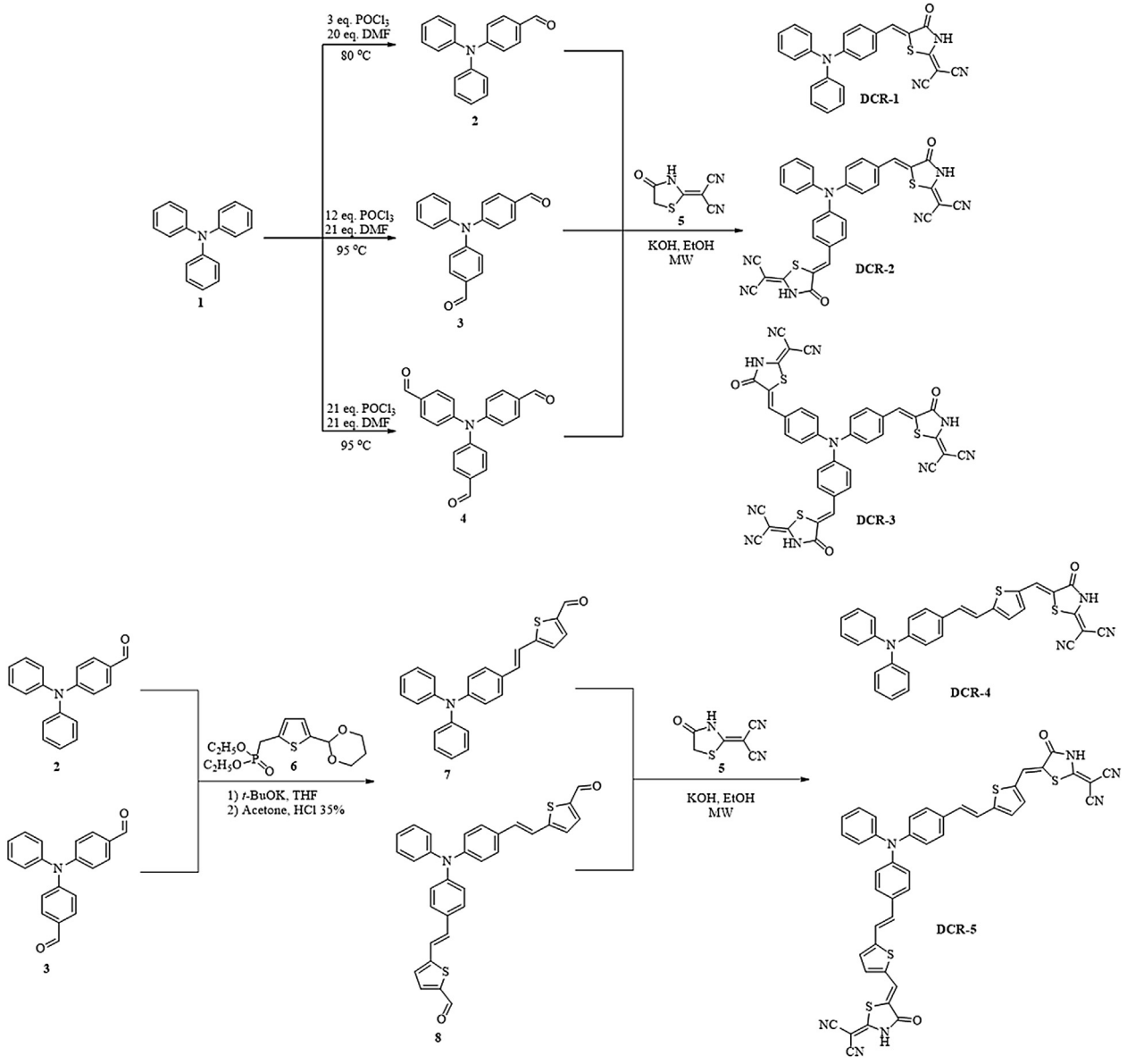

Scheme 1. Synthesis and molecular structures of dyes **DCR-(1–5)**.

spectroscopic data. FT-IR spectra of the target molecules showed the corresponding band from the NH group around 3445 cm^{-1} and the bands due to CN groups between 2209 and 2216 cm^{-1}. Moreover, the ^1H NMR spectra of these compounds showed not only the aromatic protons, but a singlet around 7.40 ppm corresponding to the olefinic proton. Furthermore, dyes **DCR-4** and **DCR-5** showed doublets corresponding to the vinyl protons around 7.39 and 7.10–7.06 ppm with a coupling constant of 16.0 Hz.

2.2. Absorption and emission properties

The absorption and emission spectra of the five **DCR-(1–5)** dyes in ethanol are shown in Fig. 1, and the data are summarized in Table 1. The absorption spectra for the dyes in solution exhibit features typical of TPA based compounds: one absorption band around 300 nm that corresponds to the $\pi \rightarrow \pi^*$ electronic transition and the other at 480 nm is the intramolecular charge transfer band between the TPA donor unit and the DCRD. It can be seen that the maximum absorption of compounds **DCR-4,5** are red-shifted in comparison to the other dyes, due to the longer π-conjugated system. The molar absorption coefficients, ε, for these dyes range from 23,400 to 93,600 M^{-1} cm^{-1} and are larger than those measured for related compounds endowed with rhodanine 3-acetic acid and cyanoacetic acid as electron acceptors [16], and for Ru-complex photosensitizers [17]. The absorption spectra for **DCR-2,3,5** displayed a long tail out to 750 nm (ε ca. 100, 500 and 800 M^{-1} cm^{-1}, respectively), suggesting the possibility of converting visible light wavelengths from 400 to 750 nm to current using these dyes.

The emission spectra for the new dyes in solution exhibit not only one distinct emission maximum, but they are generally bathochromically shifted. This effect is more pronounced in the case of **DCR-4** ($\Delta\lambda^{em}_{max}$ = 56 nm) when compared to **DCR-1** and becomes less pronounced for analogues **DCR-2** and **5**. Similarly, the maximum emission of **DCR-5** ($\Delta\lambda^{em}_{max}$ = 25 nm) is rather similar to that of its counterpart, **DCR-2**. The fluorescence quantum yields (ϕ_F) were calculated from equation (1) using *N,N*-dimethyl-6-propionyl-2-naphthylamine in EtOH (ϕ_F^{std} = 0.75) as the standard [18].

$$\phi_F = \phi_F^{std} \frac{FA^{std} In^2}{F^{std} AI^{std} n^2_{std}} \quad (1)$$

where F and F^{std} are the areas under the fluorescence curves of the dyes **DCR-(1–5)** and the standard, respectively. A and A^{std} are the respective absorbance peaks of the sample and standard at the excitation wavelengths; I and I^{std} are the relative intensities of the exciting light, and n^2 and n^2_{std} are the refractive indices of the solvents used for the sample and standard, respectively. The dyes have fluorescence quantum yields in the range of 0.0028–1.03 × 10^{-3} (Table 1). The lower ϕ_F values of the dyes show that the presence of the DCRD acceptor caused fluorescence quenching and also the presence of the thiophene linker in the dyes contributed to lower ϕ_F values.

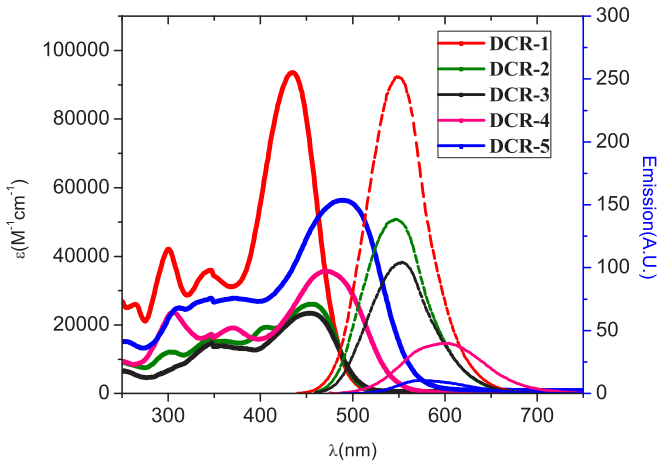

Fig. 1. Absorption and emission spectra of compounds **DCR-(1–5)** dissolved in ethanol at a concentration of 1 × 10^{-5} M.

Table 1
Photophysical properties of the synthesized dyes.

Dye	λ^{Abs}_{max}[a]/nm (ε/M^{-1} cm^{-1})	λ^{Em}_{max}[a]/nm	ϕ[b] × 10^{-3}	Stokes shift/cm^{-1}
DCR-1	435 (93,600)	548	1.03	88,496
DCR-2	455 (26,000)	547	0.62	108,696
DCR-3	454 (23,400)	554	0.10	100,000
DCR-4	471 (35,700)	604	0.073	75,188
DCR-5	489 (56,400)	572	0.0028	120,482

[a] Absorption and emission spectra were measured in ethanol solution.
[b] *N*, *N*-Dimethyl-6-propionyl-2-Naphthylamine in EtOH (ϕ_F^{std} = 0.75) was employed as the standard [18].

The corresponding absorption and emission behavior of the new dyes leads to the conclusion that these materials show strong intramolecular interactions and electronic coupling between each unit of the dye. The moiety of a triphenylamine core with a 2-(1,1-dicyanomethylene)rhodanine represents a new system with appealing push–pull properties, that could be further influenced by modifying the π-bridge unit.

2.3. Electrochemical properties

The oxidation potential (E_{ox}) corresponds to the energy of the highest occupied molecular orbital (HOMO) and the reduction potential (E_{red}) corresponds to that of the lowest unoccupied molecular orbital (LUMO). The LUMO can be calculated from the experimental values for E_{ox} (HOMO) and E_{0-0} (zero–zero excitation energy) using the equation $E_{red} = E_{ox} - E_{0-0}$. The formal redox potentials of the as-synthesized dyes were obtained by averaging the anodic and the cathodic peak potentials from the cyclic voltammogram, and the results are summarized in Table 2.

The oxidation potentials *vs* NHE were higher than that of the I^-/I_3 redox (~0.4 V *vs* NHE) couple, ranging from 0.65 to 0.87 V, ensuring that there is a sufficient driving force for efficient dye regeneration through the recapture of injected electrons from I^- by the dye cation radical [19]. The oxidation potentials for **DCR-1,2** are 0.87 and 0.84 V (*vs* NHE), respectively, indicating that the introduction of DCRD to the adjacent phenyl ring shifts the redox potentials of the dyes in a negative direction, similar to that observed for **DCR-3**. In the cases of **DCR-4,5** the addition of the vinylthiophene unit leads to a significant decrease in the oxidation potentials (up to 0.22 V *vs* NHE) when compared with **DCR-2**. This is

Table 2
Absorption–emission intersect and redox potentials (in V) of the synthesized dyes.

Dye	$\lambda_{int/nm}$	E_{0-0}[a]/eV	E_{ox} vs NHE/V	E_{red} vs NHE/V	E_{gap}[b]/V
DCR-1	486	2.55	0.87	−1.68	1.18
DCR-2	495	2.51	0.84	−1.67	1.17
DCR-3	499	2.49	0.84	−1.64	1.15
DCR-4	531	2.34	0.67	−1.67	1.17
DCR-5	541	2.29	0.65	−1.64	1.14

[a] E_{0-0} values were calculated from the intersection of the normalized absorption and the emission spectra (λ_{int}): $E_{0-0} = 1240/\lambda_{int}$.
[b] E_{gap} is the energy gap between the E_{red} of the dye and the conduction band level of TiO_2 (−0.5 V vs NHE).

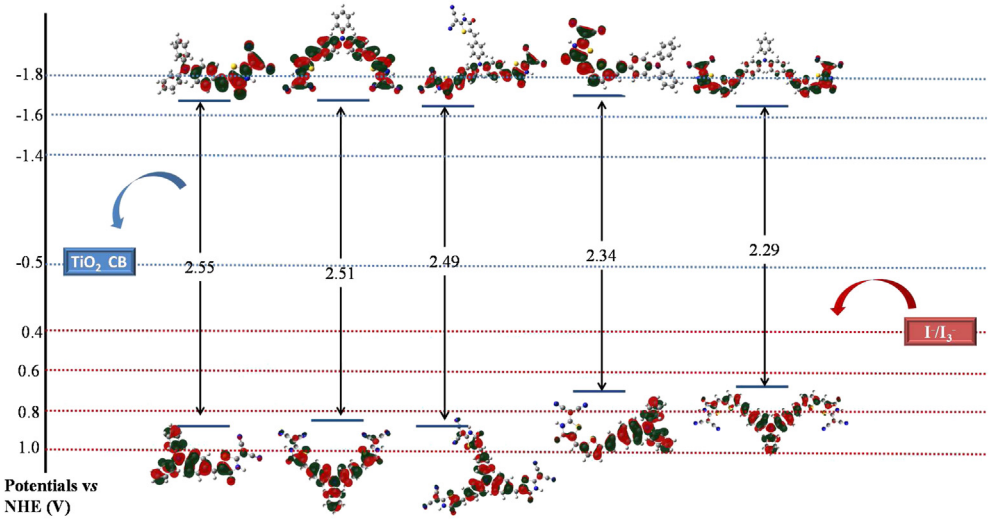

Fig. 2. Energy diagram of synthesized dyes and the frontier molecular orbitals of the HOMO and LUMO calculated with DFT at a B3LYP/6-31G + level.

due to the stabilization of the charges on the oxidized or reduced species along the conjugated chain. The estimated LUMO levels are similar for both dyes (Fig. 2) and are more than sufficient for electron injection into the TiO_2 conduction band. The higher energy of the HOMO level for **DCR-5** compared to that for **DCR-2** is therefore one explanation of the poor conversion efficiencies observed for the thiophene-based solar cells. From the data in Table 2, it can be seen that introducing DCRD to the adjacent phenyl ring of **DCR-1** to form **DCR-2** has little influence on the E_{red} (−1.68 and −1.67 V *vs* NHE, respectively), which is also observed for the other dyes.

2.4. Theoretical calculations

Density functional theory (DFT) calculations were used to shed light on the electronic structure of the novel DCRD-based organic dyes, using the Gaussian 09 program [20] and the geometries of the final products were optimized using a B3LYP functional. It is interesting to note that the position of the double-bond between TPA and the thiophene ring exists in a *trans* configuration with a dihedral angle of approximately 180°. Furthermore, it is also interesting to note the positions of the phenyl rings of the TPA, which show a starburst orientation. The compounds show a quasi-planar thiophene-acceptor union which should facilitate the electronic coupling along the molecule through the thiophene wire. As expected, the ground state energies of the calculated dyes decrease when increasing the length of the π-conjugation (Fig. 3).

We have calculated the transition state energies by means of the self-consistent field (SCF) method and polarized continuum model (PCM) in ethanol. The HOMO of the dyes is largely delocalized over the entire molecule, indicating that the binding energy of the electron in the HOMO is sensitive to a change in the π-system [21]. The LUMO is a π^*orbital mainly localized on the electron-acceptor unit of DCRD, with a minor contribution from the bridge unit (Fig. 2).

2.5. Solar cell performance

Several factors can influence the variables that contribute to the efficiency of a DSSC that include high inner resistance, light intensity, light absorption, injection efficiency, and regeneration of the oxidized dyes. The efficiency (η) of the DSSCs based on the synthesized dyes increased in the order of **DCR-4** < **5** < **1** < **3** < **2**. The DSSC based on the **DCR-2** dye shows better properties with an open circuit voltage of 0.621 V, a short circuit photocurrent density of 7.76 mA cm^{-2}, and a fill factor of 0.682, corresponding to an overall light to electricity conversion efficiency of 3.78%, which is observable in Fig. 4. The J_{sc} of the DSSCs increased in the order of **DCR-4** < **2** < **1, 3** < **5**. This could be attributed to the wider

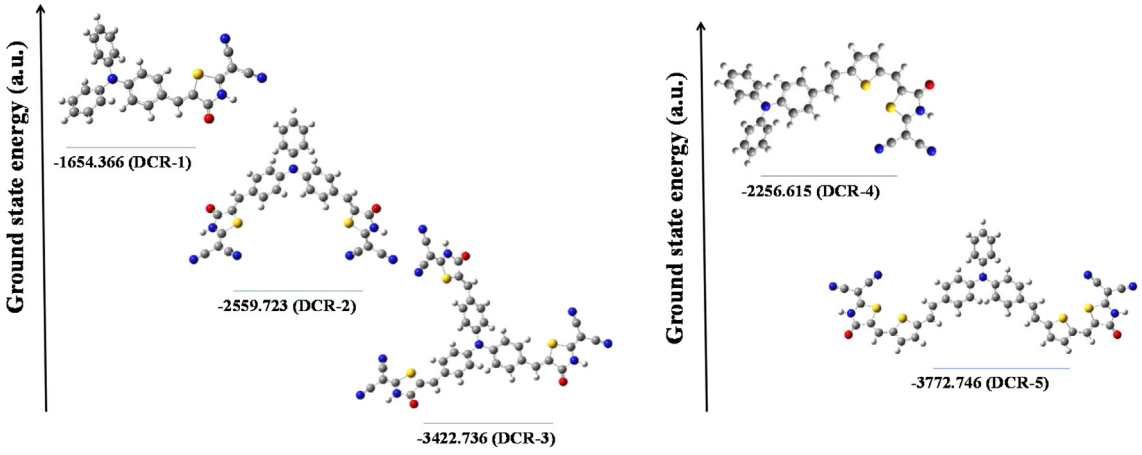

Fig. 3. Geometry optimized structures using B3LYP functional theory.

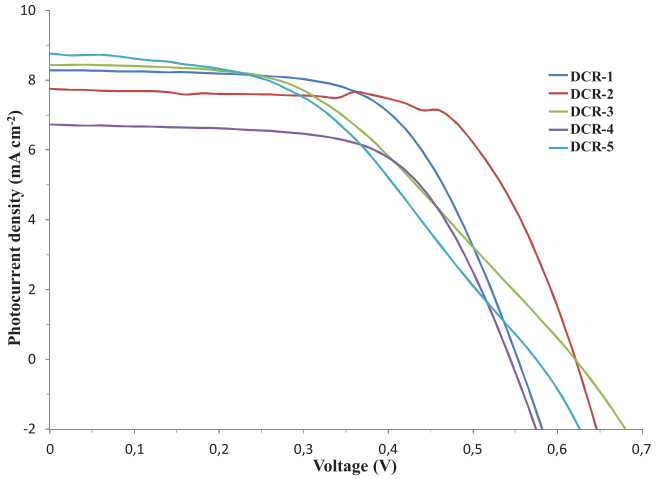

Fig. 4. *J–V* curves for DSSCs based on **DCR-(1–5)**.

Table 3
Photovoltaic parameters and performance of DSSCs from the synthesized dyes.

Dye	J_{sc}/mAcm^{-2-}	V_{oc}/V	FF	η^a (%)
DCR-1	8.28	0.553	0.62	2.92
DCR-2	7.76	0.621	0.68	3.78
DCR-3	8.28	0.592	0.66	3.44
DCR-4	6.16	0.545	0.61	2.11
DCR-5	8.76	0.575	0.46	2.37

[a] The concentration of all five dyes solutions was 3×10^{-4} M and commercially available Degussa (P25) was used for making photo-anodes. Films were dipped in all the respective dyes for 24 h.

absorption spectrum observed for **DCR-5**. Comparing the analogues **DCR-2** and **5**, it can be seen that the introduction of the thiophene unit leads to a lower fill factor, which resulted in a decreased efficiency, shown by the parameters in Table 3.

3. Conclusions

We have prepared new DCRD-based dyes for DSSCs applications using microwave synthesis. Our strategy for the dye's design is summarized by two major points: 1) the introduction of 2-(1,1-dicyanomethylene)rhodanine to replace the COOH as anchor group to the TiO_2 surface; 2) the extension of π-conjugation of the dyes tends to broaden and red-shift bands to improve the light-harvesting effect. Among these dyes, a device made with **DCR-2** exhibited the best photovoltaic results with a short-circuit photocurrent density (J_{SC}) of 7.76 mA/cm^2, an open-circuit voltage (V_{OC}) of 0.621 V, and a fill factor (ff) of 0.682, corresponding to an overall conversion efficiency of 3.78%.

4. Experimental

4.1. Materials and equipments

All solvents were dried according to standard procedures and reagents were used as purchased. All air-sensitive reactions were carried out under argon atmosphere. A CEM Discover Microwave System with an IR temperature sensor, operated by the Synergy control system software was used for microwave reactions. Flash chromatography was performed using silica gel (Merck, Kieselgel 60, 230–240 mesh or Scharlau 60, 230–240 mesh). Analytical thin layer chromatography (TLC) was performed using aluminum coated Merck Kieselgel 60 F254 plates. Melting points were determined on a Sanyo Gallenkamp apparatus. NMR spectra were recorded on a Bruker Avance 300 (^{1}H: 300 MHz; ^{13}C: 75 MHz) spectrometer at 298 K. FT-IR spectra were recorded on a Shimadzu FT-IR 8400 spectrometer. UV–Vis spectra were recorded in ethanol on a Shimadzu 1700 spectrometer. Mass spectra were recorded on a Shimadzu MS-QP 2010 spectrometer and operating at 70 eV and Matrix Assisted Laser Desorption Ionization (coupled to a Time-Of-Flight analyzer) experiments (MALDI-TOF) were recorded on a HP1100MSD spectrometer and a Bruker REFLEX spectrometer respectively. Cyclic voltammetry was performed using an Autolab PGStat 30 using a freshly polished glassy carbon working electrode (Metrohm 6.0804.010), a platinum wire as the counter electrode, and a $Ag/AgNO_3$ electrode as the reference. A 0.1 M tetrabutylammonium hexafluorophosphate ($TBAPF_6$) in dry acetonitrile was used as the supporting electrolyte. Samples were purged with argon prior to measurement at a scan rate of 100 mV/s. The Solar measurements were performed using a SS100 Photo Emission Tech Solar Simulator.

4.2. Synthesis

The starting materials 4-formyltriphenylamine (**2**), 4,4′-diformyltriphenylamine (**3**), 4,4′,4″-triformyltriphenylamine (**4**), were prepared following literature procedures [14]. Compounds **6**, 7, and **8** were prepared according to previously reported synthetic procedures and showed identical spectroscopic properties to those reported [15]. The preparation of the new DCRD-based dyes was performed by the Horner–Wadsworth–Emmons reaction followed by a Knoevenagel condensation with compound **5** under basic conditions and microwave irradiation, as shown in Scheme 1.

4.2.1. DCR-1

To an ethanol solution (2 mL) of 4-formyltriphenylamine (50 mg, 0.18 mmol) and 2-(1,1dicyanomethylene)rhodanine (45.3 mg, 0.27 mmol) 5 drops of a 5% KOH in ethanol solution was added. The mixture was then stirred under microwave conditions for 20 min. The resulting precipitate was filtered and washed with water and ethanol. The solid was purified by recrystallization from ethanol (40 mg, 52%), mp > 350 °C.

^{1}H NMR (DMSO-d_6, 400 MHz). $\delta = 7.46$ (d, $J = 8.6$ Hz, 2H), 7.42 (s, 1H), 7.34–7.38 (m, 4H),7.09–7.17 (m, 6H),6.98 (d, $J = 8.6$ Hz, 2H) ppm; ^{13}C NMR (DMSO-d_6, 100 MHz). $\delta = 180.8, 179.3, 148.1, 146.3, 130.9, 129.7, 127.6, 127.3, 126.6, 125.1, 124.2, 121.2, 118.1, 116.7, 47.1$ ppm; FTIR (KBr) $\upsilon = 3432, 2209, 1652$ cm^{-1}; MS (EI): *m/z* 420. Anal. Calcd for $C_{25}H_{16}N_4OS$: C, 71.41; N, 13.32; H, 3.84. Found: C, 71.38; N, 13.35; H, 3.96.

4.2.2. DCR-2

To an ethanol solution (2 mL) of 4,4′-diformyltriphenylamine (50 mg, 0.17 mmol) and 2-(1,1 dicyanomethylene)rhodanine (82.1 mg, 0.50 mmol) 5 drops of a 5% KOH in ethanol solution was added. The mixture was then stirred under microwave conditions for 15 min. The resulting precipitate was filtered and washed with water and ethanol. The solid was purified by recrystallization from ethanol (37 mg, 63%), mp > 350 °C.

^{1}H NMR (DMSO-d_6, 400 MHz). $\delta = 7.51$ (d, $J = 8.7$ Hz, 4H), 7.43 (s, 2H), 7.41–7.37 (m, 2H), 7.21–7.18 (m, 1H), 7.14 (d, $J = 7.7$ Hz, 2H), 7.10 (d, $J = 8.7$ Hz, 4H) ppm; ^{13}C NMR (DMSO-d_6, 100 MHz). $\delta = 180.8, 179.3, 148.1, 146.3, 130.9, 129.7, 127.6, 127.3, 126.6, 125.1, 124.2, 121.2, 118.1, 116.7, 47.1$ ppm; FTIR (KBr) $\upsilon = 3465, 2209, 1640$ cm^{-1}; MS (EI): *m/z* 595. Anal. Calcd for $C_{32}H_{17}N_7O_2S_2$: C, 64.52; N, 16.46; H, 2.88. Found: C, 64.57; N, 16.41; H, 2.98.

4.2.3. DCR-3

To an ethanol solution (2 mL) of 4,4′,4″-triformyltriphenylamine (50 mg, 0.15 mmol) and 2-(1,1 dicyanomethylene)rhodanine (112.7 mg, 0.68 mmol)5 drops of a 5% KOH in ethanol solution was added. The mixture was then stirred under microwave conditions for 15 min. The resulting precipitate was filtered and washed with water and ethanol. The solid was purified by recrystallization from ethanol (94 mg, 80%), mp > 350 °C.

^{1}H NMR (DMSO-d_6, 400 MHz). δ = 7.57 (d, J = *8.4 Hz,* 6H), 7.47 (s, 3H), 7.20 (d, J = 8.4 Hz, 6H) ppm; ^{13}C NMR (DMSO-d_6, 100 MHz). δ = 180.7, 179.3, 146.5, 132.0, 129.6, 127.9, 127.1, 124.3, 117.9, 116.5, 47.3 ppm; FTIR (KBr) υ = 3442, 2212, 1648 (C═O) cm^{-1}; MS (EI): *m/z* 770. Anal. Calcd for $C_{39}H_{18}N_{10}O_3S_3$: C, 60.77; N, 18.17; H, 2.35. Found: C, 60.73; N, 18.08; H, 2.42.

4.2.4. DCR-4

To an ethanol solution (2 mL) of aldehyde **7** (30 mg, 0.08 mmol) and 2-(1,1dicyanomethylene)rhodanine (19.5 mg, 0.12 mmol) 5 drops of a 5% KOH in ethanol solution was added. The mixture was then stirred under microwave conditions for 20 min. The resulting precipitate was filtered and washed with water and ethanol. The solid was purified by recrystallization from ethyl acetate (51 mg, 61%), mp > 350 °C.

^{1}H NMR (DMSO-d_6, 400 MHz). δ = 7.71 (s, 1H), 7.57 (d, J = 8.5 Hz, 2H), 7.49 (d, J = 4.0 Hz, 1H), 7.39 (d, J = 16 Hz, 1H), 7.36–7.33 (m, 4H), 7.27 (d, J = 4.0 Hz, 1H), 7.13–7.06 (m, 7H), 6.94 (d, J = 8.5 Hz, 2H) ppm; ^{13}C NMR (DMSO-d_6, 100 MHz). δ = 180.1, 178.3, 147.4, 147.1, 146.8, 137.7, 133.8, 130.3, 129.6, 129.2, 127.9, 127.6, 127.3, 124.4, 123.5, 122.4, 121.1, 119.8, 118.1, 116.5, 47.5 ppm; FTIR (KBr) υ = 3401, 2214, 1645, 1582, 1486, 1282 cm^{-1}; MS (MALDI-TOF): *m/z* 527.911. Anal. Calcd for $C_{31}H_{20}N_4OS_2$: C, 70.43; N, 10.60; H, 3.81. Found: C, 69.88; N, 10.65; H, 3.72.

4.2.5. DCR-5

To an ethanol solution (2 mL) of aldehyde **8** (30 mg, 0.06 mmol) and 2-(1,1dicyanomethylene)rhodanine (28.7 mg, 0.17 mmol) 5 drops of a 5% KOH in ethanol solution was added. The mixture was then stirred under microwave conditions for 15 min. The resulting precipitate was filtered and washed with water and ethanol. The solid was purified by recrystallization from ethanol (52 mg, 77%), mp > 350 °C.

^{1}H NMR (DMSO-d_6, 400 MHz). δ = 7.68 (s, 2H·), 7.58 (d, J = 8.5 Hz, 4H), 7.47 (d, J = 3.8 Hz, 2H), 7.42–7.33 (m, 4H), 7.26 (d, J = 3.8 Hz, 2H), 7.15–7.06 (m, 5H), 6.98 (d, J = 8.5 Hz, 4H) ppm; ^{13}C NMR (DMSO-d_6, 100 MHz) δ = 180.2, 178.4, 147.2, 146.6, 137.9, 133.6, 131.0, 129.7, 129.1, 127.9, 127.7, 127.5, 125.0, 123.2, 121.0, 120.1, 118.1, 116.5, 47.5 ppm; FTIR (KBr) υ = 3421, 2216, 1726, 1576, 1501, 1435 cm^{-1}; MS (MALDI-TOF): *m/z* 811.111. Anal. Calcd for $C_{44}H_{25}N_7O_2S_4$: C, 65.08; N, 12.08; H, 3.10. Found: C, 65.03; N, 12.15; H, 2.95.

Acknowledgments

The authors gratefully acknowledge financial support from COLCIENCIAS, Universidad del valle, Robert A. Welch Foundation for an endowed chair (Grant #AH-0033), U.S. Air Force grants (AFOSR-FA9550-12-1-0053 and AFOSR-FA9550-12-1-0468), and the U.S. NSF (Grant DMR-1205302). Financial support by the MEC of Spain (projects CTQ2011-24652 and Consolider-Ingenio 2010C-07-25200), the CAM (MADRISOLAR-2 project S2009/PPQ-1533) are acknowledged. N.M. and L. E. thank MINECO and NSF for funding the project PRI-PRIBUS-2011-1067.

Appendix A. Supplementary data

Supplementary data related to this article can be found at http://dx.doi.org/10.1016/j.dyepig.2014.03.010.

References

[1] Harriman A. Prospects for conversion of solar energy into chemical fuels: the concept of a solar fuels industry. Phil Trans R Soc A 2013;371:20110415.
[2] Grätzel M. Solar energy conversion by dye-sensitized photovoltaic cells. Inorg Chem 2005;44:6841–51.
[3] Hagfeldt A, Boschloo G, Sun L, Kloo L, Pettersson H. Dye-sensitized solar cell. Chem Rev 2010;110:6595–663.
[4] Yella A, Lee H-W, Tsao H, Yi C, Chandiran A, Nazeeruddin M, et al. Porphyrin-sensitized solar cells with cobalt (II/III)–based redox electrolyte exceed 12 percent efficiency. Science 2011;334:629–33.
[5] (a) Xu W, Peng B, Chen J, Liang M, Cai F. New triphenylamine-based dyes for dye-sensitized solar cells. J Phys Chem C 2008;112:874–80;
(b) Patel D, Bastianon N, Tongwa P, Leger J, Timofeeva T, Bartholomew G. Modification of nonlinear optical dyes for dye sensitized solar cells: a new use for a familiar acceptor. J Mater Chem 2011;21:4242–50.
[6] (a) Lee CW, Lu HP, Lang CM, Huang YM, Liang YM, Yen WN, et al. Novel zinc porphyrin sensitizers for dye-sensitized solar cells: synthesis and spectral, electrochemical, and photovoltaic properties. Chem Eur J 2009;15:1403–12;
(b) Campbell W, Burrell A, Officer D, Jolley K. Porphyrins as light harvesters in the dye-sensitized TiO_2 solar cell. Coord Chem Rev 2004;248:1363–79.
[7] (a) Wenger S, Bouit P, Chen Q, Teuscher J, Censo D, Humphry-Baker R, et al. Efficient electron transfer and sensitizer regeneration in stable π-extended tetrathiafulvalene-sensitized solar cells. J Am Chem Soc 2010;132:5164–9;
(b) Bouit P, Marszalek M, Humphry-Baker R, Viruela R, Ortí E, Zakeeruddin S, et al. Donor-π-Acceptors containing the 10-(1,3-dithiol-2-ylidene)anthracene unit for dye-sensitized solar cells. Chem Eur J 2012;18:11621–9.
[8] (a) Liang M, Xu W, Cai F, Chen P, Peng B, Chen J, et al. New triphenylamine-based organic dyes for efficient dye-sensitized solar cells. J Phys Chem C 2007;111:4465–72;
(b) Liang Y, Peng B, Chen J. Correlating dye adsorption behavior with the open-circuit voltage of triphenylamine-based dye-sensitized solar cells. J Phys Chem C 2010;114:10992–8;
(c) Tigreros A, Dhas V, Ortiz A, Insuasty B, Martín N, Echegoyen L. Influence of acetylene-linked π-spacers on triphenylamine–fluorene dye sensitized solar cells performance. Sol Energy Mater Sol Cells 2014;121:61–8.
[9] Ning Z, Tian H. Triarylamine: a promising core unit for efficient photovoltaic materials. Chem Commun; 2009:5483–95.
[10] Mishra A, Fischer M, Bäuerle P. Metal-free organic dyes for dye-sensitized solar cells: from structure: property relationships to design rules. Angew Chem Int Ed 2009;48:2474–99.
[11] He H, Gurung A, Si L. 8-Hydroxylquinoline as a strong alternative anchoring group for porphyrin-sensitized solar cells. Chem Commun 2012;48:5910–2.
[12] Insuasty A, Ortiz A, Tigreros A, Solarte E, Insuasty B, Martín N. 2-(1,1-dicyanomethylene)rhodanine: a novel, efficient electron acceptor. Dyes Pigments 2011;88:385–90.
[13] Mao J, He N, Ning Z, Zhang Q, Guo F, Chen L, et al. Stable dyes containing double acceptors without COOH as anchors for highly efficient dye-sensitized solar cells. Angew Chem Int Ed 2012;51:9873–6.
[14] (a) Behl M, Hattemer E, Brehmer M, Zentel R. Tailored semiconducting polymers: living radical polymerization and NLO-functionalization of triphenylamines. Macromol Chem Phys 2002;203:503–10;
(b) Yang C, Chen H, Chuang Y, Wu C, Chen C, Liao S, et al. Characteristics of triphenylamine-based dyes with multiple acceptors in application of dye-sensitized solar cells. J Power Sources 2009;188:627–34.
[15] (a) Zhang C, Harper A, Dalton L. Formylation of diethyl 2-thienylmethylphosphonate for one-pot synthesis of aminothienostilbenecarboxaldehyde. Synth Commun 2001;31:1361–5;
(b) Abbotto A, Manfredi N, Marinzi C, De Angelis F, Mosconi E, Yum JH, et al. Di-branched di anchoring organic dyes for dye-sensitized solar cells. Energy Environ Sci 2009;2:1094–101.
[16] (a) Tian Z, Huang M, Zhao B, Huang H, Feng X, Nie Y, et al. Low-cost dyes based on methylthiophene for high-performance dye-sensitized solar cells. Dyes Pigments 2010;87:181–7;
(b) Abbotto A, Manfredi N, Marinzi C, De Angelis F, Mosconi E, Yum JH, Xianxi Z, Nazeeruddin M, Grätzel M. Di-branched di anchoring organic dyes for dye-sensitized solar cells. Energy Environ Sci 2009;2:1094–101.
[17] Nazeeruddin M, Zakeeruddin SM, Humphry-Baker R, Jirousek M, Liska P, Vlachopoulos N, et al. Acid–base equilibria of (2,2'-Bipyridyl-4,4'-dicarboxylic acid)ruthenium(II) complexes and the effect of protonation on charge-transfer sensitization of nanocrystalline titania. Inorg Chem 1999;38(26):6298–305.
[18] Williams A, Winfields S. Relative fluorescence quantum yields using a computer-controlled luminescence spectrometer. Analyst 1983;108:1067–71.
[19] Tian H, Yang X, Chen R, Zhang R, Hagfeldt A, Sun L. Effect of different dye baths and dye-structures on the performance of dye sensitized solar cells based on triphenylamine dyes. J Phys Chem C 2008;112:11023–33.
[20] Frisch MJ, Trucks GW, Schlege HB, Scuseria GE, Robb MA, Cheeseman JR, et al. Gaussian 03, Revision C.02. Wallingford CT: Gaussian, Inc.; 2004.
[21] Qin P, Yang X, Chen R, Sun L, Marinado T, Edvinsson T, et al. Influence of π-conjugation units in organic dyes for dye-sensitized solar cells. J Phys Chem C 2007;111:1853–60.